

Figure S1. Kir 2.6 Mutations Found in Our TPP Cohort and Their Conservation across Species—Related to Figure 1

A total of six mutations were found in our cohort of TPP patients. Chromatograms from mutations with R205H, T354M, K366R, R399X, Q407X, and I144fs (versus wild-type) are shown. The missense mutations (R205H, T354M, and K366R) are at residues that are well conserved both among human Kir2 family members as well as across other species (position of the mutation is underlined).

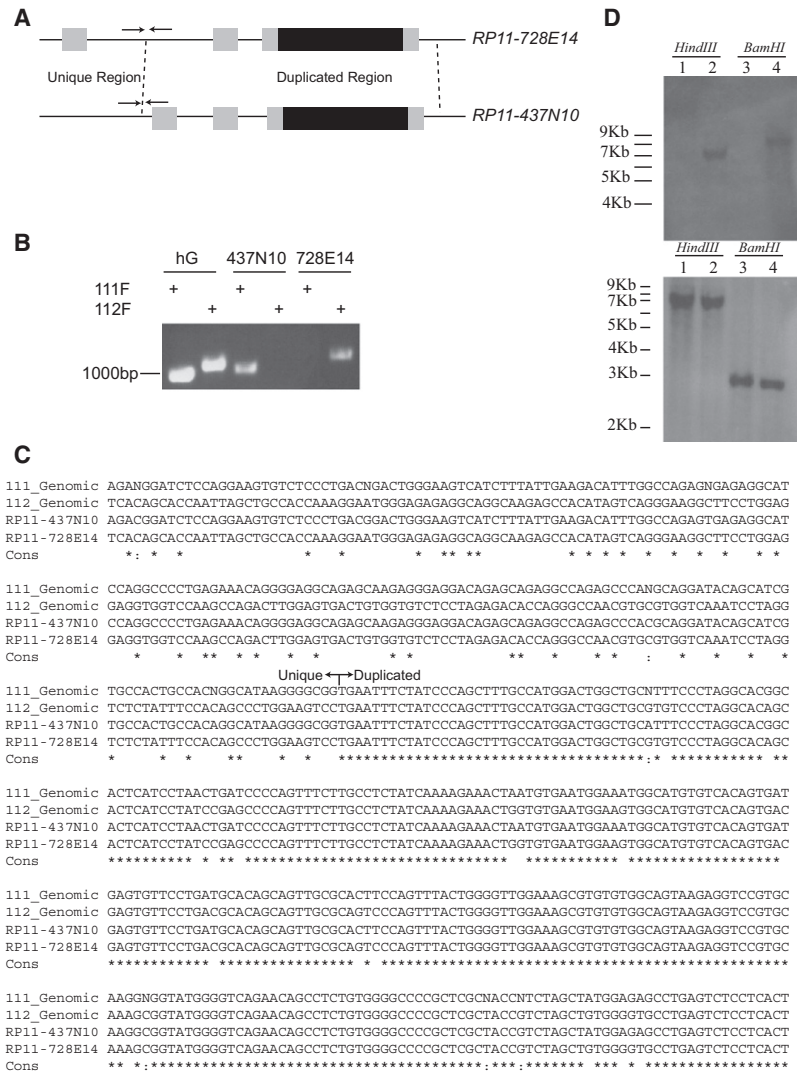


Figure S2. *KCNJ18* and *KCNJ12* Are Unique—Related to Figure 2

Alignment of the BACs containing *KCNJ12* (RP11-728E14) and *KCNJ18* (RP11-437N10) suggests that *KCNJ18* is largely a duplication of *KCNJ12* (A, diagram as in Figure 1 where dashed lines indicate duplication boundaries and arrows primer position). The duplication/unique region boundary can be specifically amplified from each BAC using a specific forward primer (111F: CCCAATCAAGCAGAAACACA or 112F: CCTGCTAGATCCCAGCTCAG) and a non-specific reverse primer (111R: GGAGAAACCGGAGAAACACA), indicating that the BACs are unique (B). Both primer pairs are also able to produce different PCR products from human genomic DNA (hG). Alignment of the sequence of both BAC and human genomic PCR products indicates that the amplicons from an individual primer pair match between BAC and human genomic DNA, but not between primer pairs except in the duplicated region (C). A portion of the sequence is shown for both genomic DNA (111_Genomic or 112_Genomic for amplicon from 111F or 112F primer, respectively) and BAC DNA is shown. N indicates the presence of a polymorphism. Cons shows the conservation between all four sequences with a "*" indicating 100% conservation and a ":" indicating at least partial conservation, due to a polymorphism. The boundary of the unique and duplicated region is indicated. PCR from genomic DNA was performed with the same method used to screen for TPP mutations. BAC PCR was performed using Phusion DNA polymerase (Finnzymes, MA) according to the manufacturers instructions. Digested BAC DNA was probed with biotinylated synthetic probe targeted against either the unique exon 1 (CTGTTGGGAAGCCTGTTTC/ GTCACGAGGTAAGCCAAGC, D top) or the conserved exon 3 (CAACCCCTACAGCATCGTGTGC/TCCACACAGGTGGTGAACAT, D bottom). Both BACs were digested with BamHI or HindIII for 16 hr prior to fractionation. BAC RP11-728E14 was (digested as indicated) was run on lanes 1 and 3 while BAC Rp11-437N10 was run on lanes 2 and 4. Blots were performed simultaneously from the same digested DNA and gel. Expected sizes, according to reference BAC sequence, were: 0bp, D top 1; 7174bp, D top 2; 0bp, D top 3; 8408bp, D top 4; 6589bp, D bottom 1; 6572bp, D bottom 2; 2583bp, D bottom 3; 2583bp, D bottom 4.

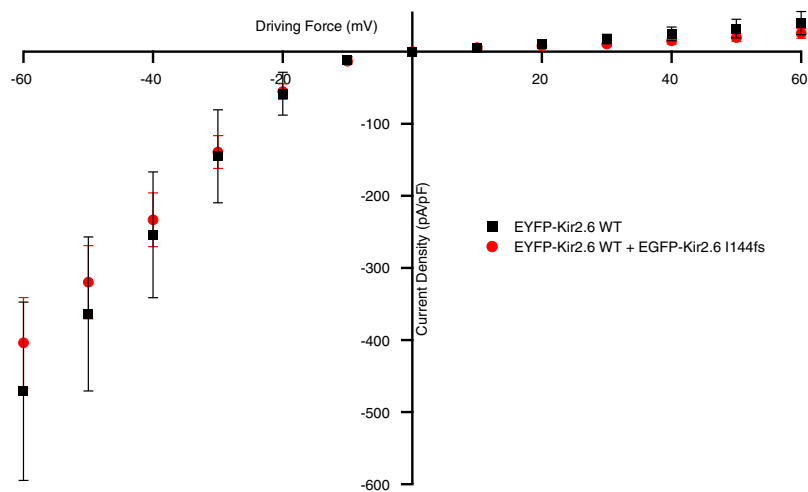


Figure S3. The I144fs Mutation Does Not Act in a Dominant Negative Manner—Related to Figure 4

Wild-type (black squares) channels were expressed in HEK293 cells at half their normal levels with or without an equivalent amount of I144fs mutant (red circles for WT + I144fs). Voltage steps indicate that the wild-type current is unaffected by coexpression of the I144fs (wild-type = -471.074 ± 123.65 pA/pF and cotransfected = -402.898 ± 62.69 pA/pF at -60 mV).

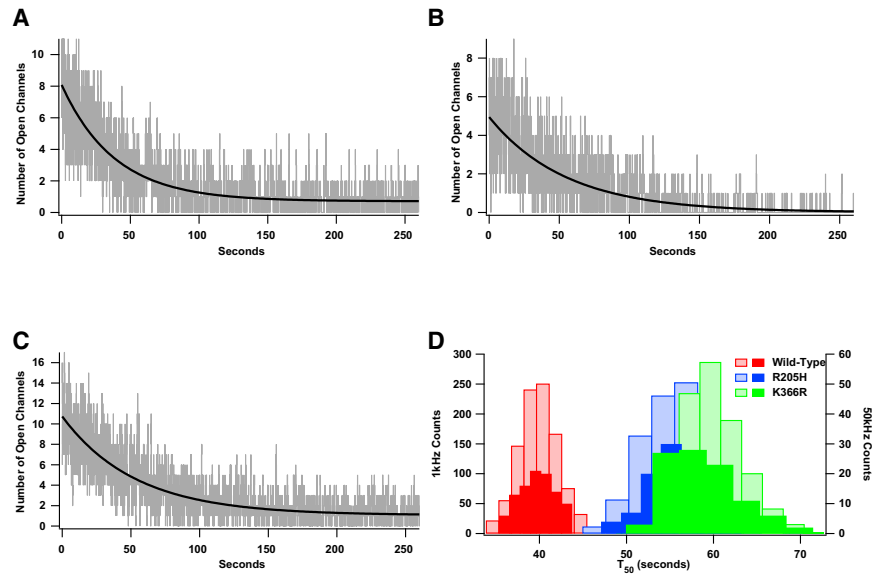


Figure S4. Statistical Modeling of Ion Channel PIP2 Interactions Indicates Robustness of T_{50} Estimations—Related to Figure 6

Individual idealized ion channel open and closed states were simulated in accordance to fit parameters from Figure 6. Open state dwell times were randomly selected from an exponential distribution with mean 220ms. Closed state dwell times were randomly selected from a similar distribution whose mean was altered over time such that the mean open probability would follow the curve fit from Figure 6. Initial open probability for each channel type was also taken from Figure 6 (0.65 for wild-type, 0.55 for R205H mutant, or 0.49 for K366R mutant). For each run, 11 (wild-type, A), 9 (R205H mutant, B) or 19 (K366R mutant, C), idealized openings were summed and fit with an exponential function as in Figure 6. Simulations were sampled at either 1kHz or 50kHz and the values derived from their fit stored and displayed as a histogram (D, light bars are 1kHz simulations and dark bars are 50kHz simulations). 1000 (1kHz sampling) or 100 (50kHz sampling) runs of each simulation were performed for each channel. The resulting T_{50} values have means 39.82 ± 0.07 s or 39.65 ± 0.20 s (Wild-type sampling 1kHz or 50kHz, respectively), 55.96 ± 0.13 s or 55.58 ± 0.34 s (R205H mutant 1kHz or 50kHz sampling, respectively), and 59.67 ± 0.11 s or 58.63 ± 0.40 s (K366R mutant 1kHz or 50kHz sampling, respectively). Simulations were run in Igor Pro (Wavemetrics). Similar results are seen if dwell times are chosen from Gaussian or gamma distributions (not shown).